Journal of Power Sources 193 (2009) 788–796

Contents lists available at ScienceDirect

Journal of Power Sources

journal homepage: www.elsevier.com/locate/jpowsour

Development and demonstration flight of a fuel cell system for high-altitude balloons

Masatoshi Uno[a,*], Takanobu Shimada[a], Yusuke Ariyama[b], Naoya Fukuzawa[b], Daisuke Noguchi[b], Keita Ogawa[c], Hitoshi Naito[d], Yoshitsugu Sone[a], Yoshitaka Saito[a]

[a] Institute of Space and Astronautical Science, Japan Aerospace Exploration Agency, 3-1-1 Yoshinodai, Sagamihara, Kanagawa 229-8510, Japan
[b] Hosei University, Koganei, Tokyo 184-8584, Japan
[c] Advanced Engineering Services, Tsukuba, Ibaraki 305-0032, Japan
[d] Aerospace Research and Development Directorate, Japan Aerospace Exploration Agency, Tsukuba, Ibaraki 305-8505, Japan

ARTICLE INFO

Article history:
Received 27 February 2009
Received in revised form 27 April 2009
Accepted 8 May 2009
Available online 20 May 2009

Keywords:
Fuel cell
Balloon
High altitude
Demonstration flight
Back pressure regulator

ABSTRACT

Proton exchange membrane fuel cell offers higher energy density than the existing battery technologies for high-energy applications, and it is a promising power source for various industries including aerospace vehicles. We have been developing and testing a non-external humidified fuel cell system for high-altitude balloons, which require simple, light, and easy-to-operate power systems. This system consists of three major subsystems—a fuel cell stack, a reactant supply subsystem, and an electrical control subsystem. Ground performance testing in a vacuum chamber simulating the high-altitude vacuum condition was performed before the flight. Then, a demonstration flight of the fuel cell system was launched using a large balloon for verifying its performance under practical high-altitude conditions. Cell voltage variations synchronized with oxygen pressure spikes were observed that were probably caused by condensed product water plugging the flow passages of the back pressure regulator. Flight results indicated that the fuel cell system operated better when water was expelled as vapor, rather than in the liquid form. In addition, a back pressure regulator should be installed to avoid the accumulation of water droplets for realizing a stable performance.

1. Introduction

Fuel cells, which convert chemical energies of reactants to electrical energy, are considered to be one of the most viable next generation power sources. In general, it is widely accepted that the proton exchange membrane fuel cell (PEMFC) is the most likely alternative to the internal combustion engine of automobiles. In addition, PEMFCs have drawn attention as a promising technology for mobile and portable applications due to their low-temperature performance and high-energy densities. Because PEMFCs can achieve much higher specific energy densities than any of the advanced battery technologies, the aerospace industry is considering their application in aerial vehicles [1–4].

PEMFC also has the potential to be a power source for high-altitude scientific and engineering balloons, as shown in Fig. 1, for which simple, light, reusable, low-cost, and easy-to-operate systems are required. Current Japanese balloon systems employ lithium primary batteries as their power sources, because they offer higher energy densities than the other types of battery technologies. However, reusable/rechargeable power sources are strongly desired recently in order to reduce the cost of replacing the primary batteries for every flight. Besides, lithium primary battery is no longer the lightest power source for high-energy missions and long term flights. Current balloon systems using lithium primary batteries will find it difficult to meet an increasing demand for high-energy missions in terms of reusability and cost-effective operation. PEMFCs might be the best solution for these increasing demands. Although PEMFCs offer advantages for balloon systems, several major challenges must be overcome with respect to the system complexity and operation at high altitude.

Proton exchange membranes (PEM) show high ionic conductivity only under well-hydrated conditions, and this is necessary for an efficient and stable operation. Product water can be utilized for self-humidification. In general, however, this is not enough to realize well-hydrated condition for PEMFC systems using air as an oxidant. Air contains nitrogen which is inactive to reactions and accounts for four-fifth of air. Nitrogen decreases the partial pressure of vapor that directly determines the relative humidity at a given temperature and production rate of water, namely hydration level of the membrane [5]. Therefore, reactant gases such as hydrogen and the air should be humidified before being introduced in order to provide an adequate relative humidity with which PEM-

* Corresponding author. Tel.: +81 42 759 8366; fax: +81 42 759 8366.
E-mail address: uno.masatoshi@isas.jaxa.jp (M. Uno).

0378-7753/$ – see front matter © 2009 Elsevier B.V. All rights reserved.
doi:10.1016/j.jpowsour.2009.05.010

Fig. 1. A photograph of a high-altitude balloon.

FCs can be stable and operate efficiently. However, this requires an external humidification equipment that increases the weight, volume, and complexity of PEMFC systems. Aerospace vehicles, such as rockets, satellites, and high-altitude balloons require simple and light systems to reduce their mass and the risk of failures. Because the ambient temperatures of such vehicles are generally lower than terrestrial applications, humidification equipment that usually contains a large amount of water requires a large amount of heat to warm the water sufficiently. Unless the thermal design is correct, the vapor in the reactant gases might be condensed or frozen before being supplied to the fuel cell at a low ambient temperature. Thus, non-external humidified operation is preferred for aerospace applications.

It is well known that counter-flow orientation, which orients the anode and cathode flow in opposite directions, is the preferred method of self-humidification. This technique utilizes the product water formed in the cathode exit to humidify the anode inlet so as to perform the non-external humidified operation [6–8]. Another possible method is to use customized flow fields to balance the moisture distribution [9].

For aerospace vehicle applications, the effect of a decreasing ambient pressure with altitude on the PEMFC performance must be considered. According to the Nernst equation that expresses the theoretical potential of fuel cell, a decrease in oxygen partial pressure with an increase in altitude plays a significant role in changing its performance. In addition, vacuum at high altitudes decreases both the oxygen partial pressure and vapor pressure that determines the relative humidity at a given temperature. A low vapor pressure leads to severe dryness preventing the PEM from sustaining high ionic conductivity. Operating pressures of PEMFCs should be maintained within a particular range to achieve sufficient performance and a continuous operation.

A fuel cell bus, equipped with 20 stacks, each providing 13 kW power, was operated at a high altitude in Mexico City (more than 2240 m above sea level) where the air is 25% thinner than that in Vancouver (at sea level), resulting in a poorer performance, because the air compressor was not able to provide enough oxygen to the fuel cell stacks [10]. Pratt et al. investigated the impact of altitude on PEMFC performance for aerospace relevant high-altitude conditions [11]. The previous studies suggested that high altitude inevitably leads to a significant performance loss caused by a decreased cathode pressure and oxygen concentration, as long as PEMFCs were designed to use air as its cathode reactant.

We have been developing a non-external humidified PEMFC system using pure oxygen as an oxidant, which utilizes product water for self-humidification [8,12]. In this study, a PEMFC with back pressure regulators (BPR), maintaining the operating pressure higher than a particular value, was developed for a demonstration flight using a high-altitude balloon. Prior to the demonstration flight, ground tests were performed emulating the stratospheric conditions. The system was equipped with a B50-50 balloon, 50th B-50 model balloon (50,000 m^3 of volume), and was launched from the Sanriku Balloon Center (SBC) on August 30th, 2007 to verify its performance in an actual high-altitude environment where the atmospheric density and temperature are very low.

2. The fuel cell system

The fuel cell system consists of three major subsystems—a fuel cell stack, a reactant supply subsystem, and an electrical control subsystem.

2.1. Fuel cell stack

A self-developed PEMFC stack, consisting of 16 cells with an active area of 162 cm^2 each, was used. Bipolar graphite plates for both the anode and cathode had triple serpentine flow fields that are each 1.25 mm wide and 1.20 mm deep. Commercially available membrane electrode assemblies (MEA) (Japan GORE-TEX, GORE™ PRIMEA® 5510, 30 μm), and gas diffusion media with micro-porous layers (Japan GORE-TEX, CARBEL®-CFP 400) were employed. The fuel cell stack was fed in counter-flow mode with non-humidified hydrogen and oxygen from a reactant supply subsystem.

A fuel cell stack weighing 18.6 kg was developed as a 1 kW class for in-house performance tests [12]. Therefore, it was not optimized to maximize its energy/power density for the demonstration flight. In general, fuel cells are cooled to remove the product heat corresponding to a power generation loss. The stack was designed to control its temperature using coolant water; however, active temperature control using coolant water was not employed for the demonstration flight, because the fuel cell system was designed to be as simple as possible. Instead of active temperature control, the stack was thermally insulated to maintain it at an appropriate temperature. Because the fuel cell system could be exposed to very cold ambient conditions at high altitude (−50 °C at the coldest) and was supposed to be operated at a low power of 50 or 80 W which was less than one-tenth of its intrinsic performance, the stack must be insulated for self-heating. In this system, the stack temperature was same as the ambient temperature (20–30 °C) at the beginning of the operation and gradually increased as time elapsed. This temperature profile was preferable for non-external humidified operation. Although the reactants were supplied without humidification, the relative humidity of the stack would be sufficient to sustain a stable operation, because the saturated vapor pressure is low at low temperature. After the fuel cell stack was warmed by its power generation loss, an excess of product water accumulated in the stack

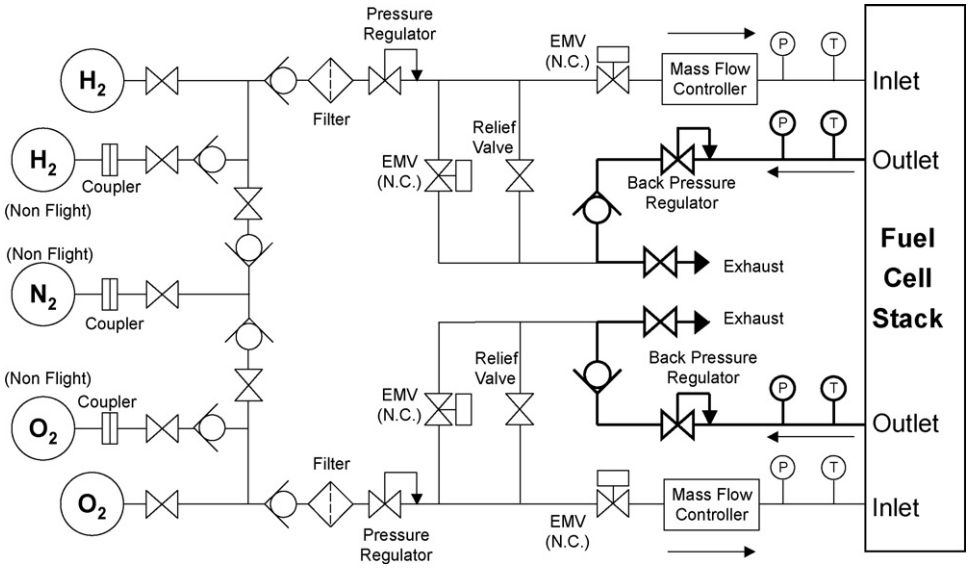

Fig. 2. Schematic of the reactant supply subsystem for the fuel cell system.

could be removed as the saturated vapor pressure increased with the temperature.

2.2. Reactant supply subsystem

For closed environmental systems, which do not exhaust reactants to the outside, or for systems aiming for high-energy utilization, reactants that did not react in the fuel cell must be recirculated back to the inlet of the fuel cell for minimizing the wastage of reactant gases [8,12]. Such systems require recirculation equipment, such as a diaphragm pump, chemical pump [13], or ejector [14], thereby increasing the cost, complexity, and control difficulty. In this study, from the perspectives of simplicity and facilitation of operation, we employed a non-recirculation system, focusing on the implementation of the demonstration flight, and a recirculation system is left for future work.

Fig. 2 shows a schematic drawing of the reactant supply subsystem. Unreacted hydrogen and oxygen were exhausted through the BPRs. If the inside of the fuel cell stack was exposed to vacuum at high altitudes, evaporation of an extreme amount of water would make stable operation impossible. BPRs (TESCOM, 44-47, 50 psig) maintained the operating pressure of the fuel cell stack above the ambient pressure to avoid an extreme evaporation of water in the MEAs.

Gas cylinders with an internal volume of 2.8 and 2.0 L (JFE Container, ACB 2.8 and ACB 2.0) were used as sources for hydrogen and oxygen, respectively. The fuel cell stack used these gases to generate electricity during the entire demonstration flight. The cylinders were made of an aluminum–carbon fiber-reinforced plastic, and their maximum pressures were 19.6 MPa. Non-flight cylinders were connected in parallel via check valves to the flight cylinders to reduce gas consumption before the launch. Hydrogen and oxygen were fed by either external or internal supplies. The fuel cell system was operated with an external supply using non-flight cylinders during ground tests, and was switched to an internal supply using flight cylinders before the launch. The gas supply could be switched by stop valves and check valves.

The fuel cell system was supposed to be exposed to very cold ambient conditions (−50 °C) at high altitude, and freezing of product water in the fuel cell was expected to deteriorate its performance. The fuel cell stack was thermally insulated, as mentioned in Section 2.1. Freezing in the piping after the outlets of the fuel cell stack might block the flow of reactants. The parts placed between the outlets of the fuel cell stack and exhaust ports, such as piping, check valves, manual valves, and BPRs, depicted by thick lines in Fig. 2, were warmed by heaters to prevent the freezing of product water at high altitudes. Thermal vacuum tests, simulating high-altitude cold and subatmospheric ambient pressure conditions, were conducted to verify the tolerance against low temperature before the flight. Based on the results of the thermal vacuum test, heater resistance values were determined experimentally that would keep the temperatures of these parts above 0 °C even in the coldest ambient condition (−50 °C).

The fuel cell system must be vacuum-tolerant, because it is exposed to vacuum at high altitudes. Traditional mass flow controllers using thermal principles for determining mass flow rates do not work under subatmospheric conditions, because the thermal conditions under normal pressure are totally different from those at subatmospheric conditions where there is less heat convection. Mass flow controllers (ACE, AFC-150) that detect pressure drops between laminar tubes to determine the mass flow rates were used in place of traditional controllers.

For emergency operations, electromagnetic valves (EMVs) were placed between the fuel cell stack and cylinders to stop the reac-

Fig. 3. A photograph of the fuel cell stack installed in the reactant supply subsystem.

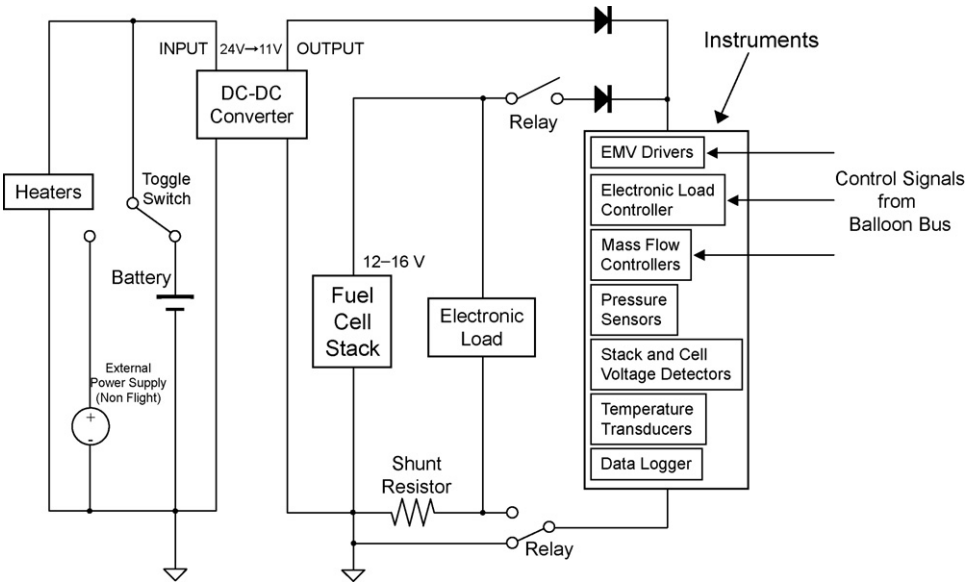

Fig. 4. Schematic representation of the electrical control subsystem.

tant supply. EMVs placed between the cylinders and exhaust ports exhaust the residual gas in the cylinders after the termination of the demonstration flight. The balloon was supposed to land on the sea using a parachute after completing the mission for recovery operation. If the reactants remained in the cylinders, there could be leakage followed by a possible explosion, because the shock of landing might damage the gas cylinders and piping. The residual reactant exhaustion operation was executed to assure safety from a possible explosion during recovery operations. The EMVs could be operated by sending a command from the ground.

Fig. 3 shows a photograph of the fuel cell stack installed in the reactant supply subsystem. The stack was oriented horizontally. The system had a mass of 40 kg (including the fuel cell stack weighing 18.6 kg) with dimensions of 50 cm × 50 cm × 60 cm. The fuel cell system could be made much smaller and lighter if the fuel cell stack was optimized for the flight.

2.3. Electrical control subsystem

Fig. 4 shows a schematic representation of the electrical control subsystem. This subsystem consists of EMV drivers, an electronic load, mass flow controllers, sensors, transducers, a data logger, heaters, and a battery.

The electrical control subsystem must be powered by a power source other than the fuel cell stack during the startup procedure for introducing hydrogen and oxygen into the fuel cell stack using mass flow controllers and EMVs. At the beginning of the startup procedure, the subsystem was powered with an external power supply or battery via the dc–dc converter providing 11 V, which is slightly less than the nominal voltage range of the fuel cell stack (12–16 V), and the fuel cell stack output was directed only to the electronic load. After switching power relays and completing the startup, the fuel cell stack provided output to both the electronic load and flight instruments. Because the output terminals of the fuel cell stack and the dc–dc converter were connected in parallel via diodes, the subsystem was never shut down, even at the moment of switching the power relays. At that time, all flight instruments other than heaters were powered by the fuel cell stack. The battery operated as a back-up power source in case of an abnormal situation, such as failure of the fuel cell stack to generate enough power. The heaters alone were designed to be powered directly by the battery, because the heaters must be powered under all circumstances in order to warm the tubes and valves placed lower than the fuel cell stack in order to prevent the freezing of product water with which the residual reactant gases cannot be exhausted before landing on the sea.

The EMV status, mass flow rates, and the load current could be changed by sending commands from the ground. Control signals converted from the command signals were sent to these instruments from the balloon bus, which is outside the scope of this paper.

3. Flight sequence and operating conditions

3.1. Flight sequence

Fig. 5 shows the sequence of the demonstration flight. Startup procedure took 0.5 h. This was empirically determined to achieve a 50 W power generation. The fuel cell continued generating during the helium filling operations following the launch. After reaching an altitude of 35 km, the balloon maintained the altitude and shifted to horizontal flight by dropping the ballast. Two hours before landing (the end of the demonstration flight), the power generation was increased to approximately 80 W by sending a command.

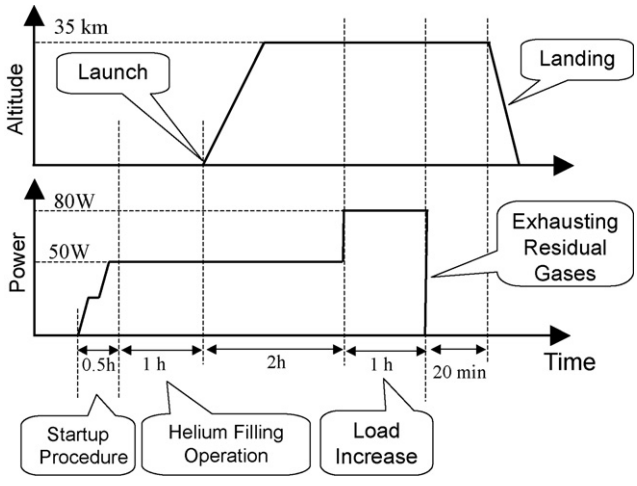

Fig. 5. Sequence of the demonstration flight.

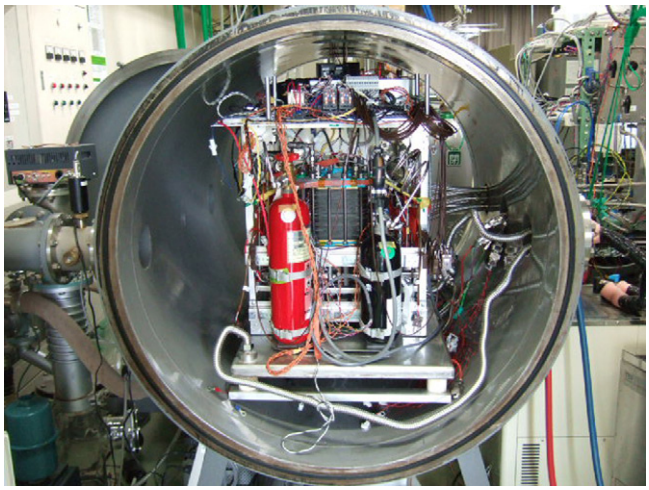

Fig. 6. A photograph of the fuel cell system in the vacuum chamber.

The numbers in Fig. 5 are approximate values that were supposed to change according to the situation.

3.2. Startup procedure and operating condition

Non-flight gas cylinders and an external power supply were used during the startup procedure to economize the reactants and battery energy. The reactants, hydrogen and oxygen, were introduced after the fuel cell stack was purged with nitrogen for more than 5 min. After a sufficiently high open-circuit voltage (OCV) was obtained, the fuel cell stack was operated with a load current of 2 A for 10 min, and subsequently at 4 A, corresponding to a power generation of approximately 50 W. The balloon was launched after being filled with helium. The load current was increased to 7.5 A, corresponding to about 80 W power, with a command sent from the ground after the balloon had attained a horizontal flight. The operating pressure of the fuel cell stack was set to approximately 100 kPa (gauge) using the back pressure regulators so that the operating pressures were maintained at 201.3 and 101.3 kPa (absolute) under atmospheric and high-altitude conditions, respectively. In other words, the operating pressure was always 100 kPa higher than the ambient pressure. Hereafter, all pressure values are expressed in terms of absolute pressure. The stoichiometries of hydrogen and oxygen were set to 2 and 3, respectively, with which the reactants in the flight cylinders were fully consumed with a margin of at least 1 h operation. With these stoichiometries, the residual reactant exhaustion operation could be shortened and its risk of failing could be mitigated by leaving small amounts of reactants at the end of the flight.

4. Results and discussion

4.1. System ground test

To verify the vacuum-tolerant performance of the fuel cell system, before the demonstration flight, system-level ground tests were performed using a vacuum chamber. Fig. 6 shows a photograph of the fuel cell system placed in the vacuum chamber. The fuel cell stack was not thermally insulated during the ground test, because the ambient temperature of the ground test, that is the room temperature, was completely different from the stratospheric conditions (−50 °C at the coldest). A rotary pump reduced the vacuum to about 1 kPa, which was enough to simulate the stratospheric vacuum level. Reactants that were not reacted in the fuel cell stack were exhausted to the atmosphere through a flange so that secondary pressures of the BPRs were always 101.3 kPa in the ground tests. However, the secondary sides of the BPRs had to be exposed to vacuum at a high altitude. Bringing the secondary sides to a subatmospheric pressure was necessary in order to confirm the performance of the BPRs. A direct evacuation of hydrogen and oxygen using a vacuum pump was not considered appropriate due to the possibility of an explosion inside the pump, which contained the lubricant.

A temporary vacuum system consisting of 3-way valves and buffer tanks, as shown in Fig. 7, was connected to the exhaust ports

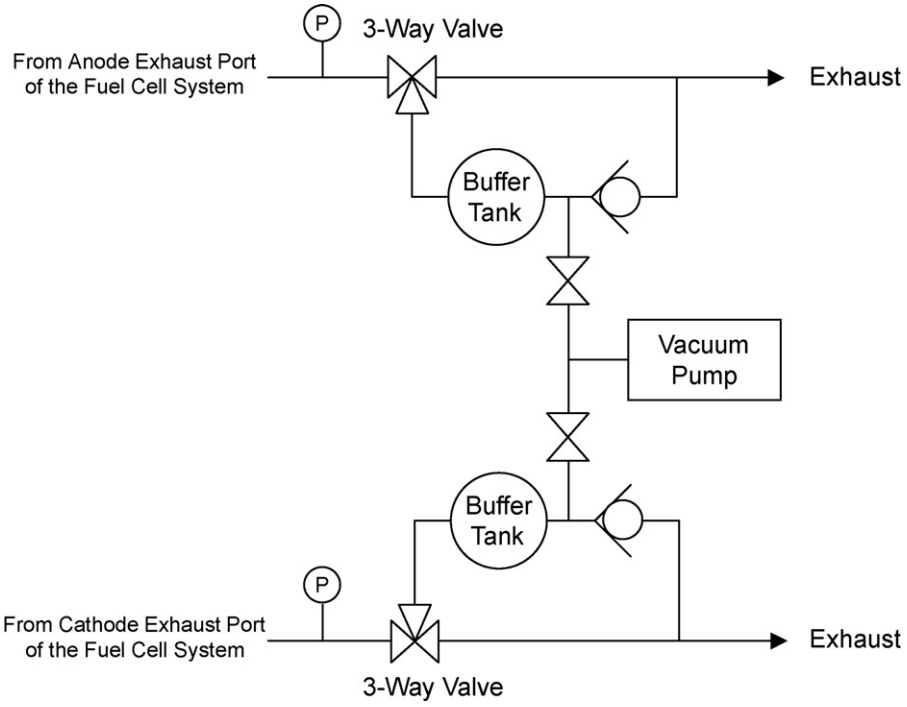

Fig. 7. Temporary vacuum system for the ground tests.

of the fuel cell system instead of direct evacuation. Normally, reactants directly go through the 3-way valves to the exhaust ports of the temporary vacuum system, whereas the buffer tanks are evacuated by a vacuum pump. When the directions of the 3-way valves are switched, the pre-vacuumed buffer tanks and secondary sides of the BPRs are directly connected so that the secondary pressures of the BPRs immediately drop to subatmospheric pressure. After switching, the secondary pressures increase linearly, as long as the outlet flow rates are constant. Reactants flow into the buffer tanks until the pressures of the buffer tanks exceed the cracking pressures of check valves followed by the exhaustion through the check valves. Finally, the 3-way valves were switched back to separate the buffer tanks filled with the reactants.

Fig. 8 shows the results of the ground performance test performed in the vacuum chamber. At the beginning of the test, some cell voltages showed an unstable performance which was thought to be caused by flooding due to an insufficient purging before the test, as shown in the top of Fig. 8. The operating temperature was rather low at the beginning of the test, as shown in the bottom of Fig. 8. In addition, water was presumably accumulated inside the fuel cell stack in the previous test after which the purging was insufficient; therefore, the fuel cell stack showed a flooding-prone performance requiring sufficient purging before the test. The performance became stable, because the excess water was removed by increasing stack temperature, as mentioned in Section 2.1.

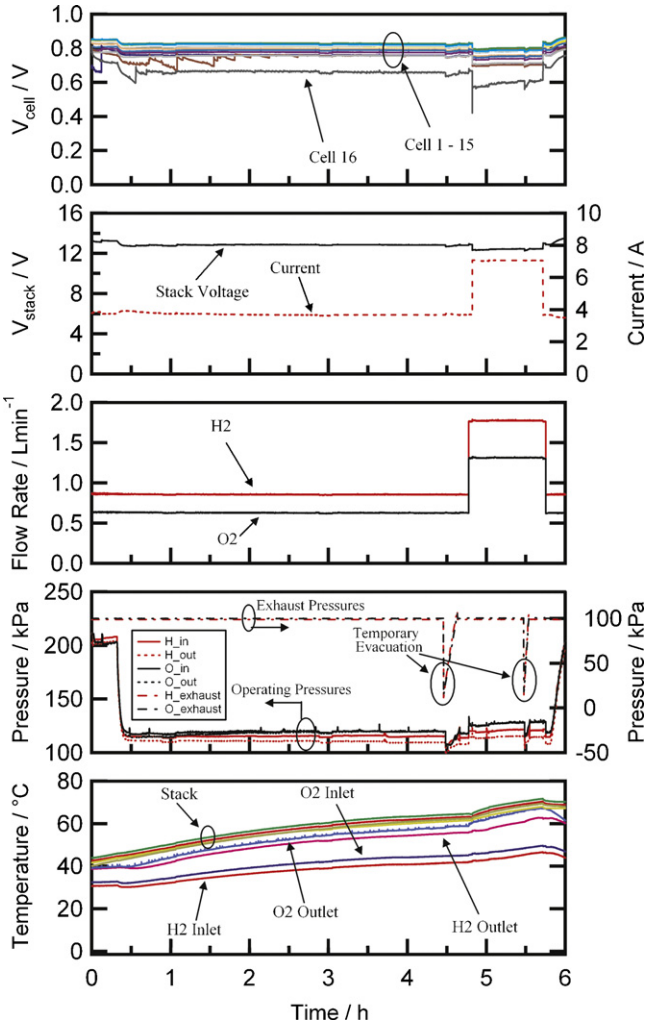

Fig. 8. Performance of the fuel cell system during the ground test. From the top to the bottom, cell voltage, stack voltage or load current, flow rate, stack pressure, or exhaust pressure, and temperature are plotted.

Evacuation of the chamber was started 20 min after the start of the test, as shown in the second figure from the bottom in Fig. 8. As the evacuation proceeded, operating pressures immediately decreased along with a decrease in chamber pressure. Since the operating pressures were regulated by BPRs whose performances slightly depend on secondary pressure, the operating pressures were stable at around 120 kPa which was slightly higher than the set value of 100 kPa, when the exhaust pressures were atmospheric. Since the fuel cell voltages depend on operating pressures, the decreases in operating pressures caused slight decreases in stack and cell voltages. Cell 16 showed the worst performance—this had been observed prior to the test. This was presumably caused by the stack assembly related problems which were not correlated with the vacuum condition of the ground test.

The temporary vacuum was executed twice, i.e., before and after increasing the load current. An abrupt evacuation of the secondary sides of the BPRs caused slight decreases in the operating pressures. Immediately after switching to temporary evacuation, the operating pressures were almost 100 kPa, indicating an appropriate performance of the BPRs. The operating pressures recovered to approximately 120 kPa when the exhaust pressure returned to 100 kPa. Since the BPRs have the trait of accumulation [15], which is an increase in primary pressure as the flow increases, the operating pressures slightly rose after increases in the mass flow rates of the reactants followed by doubling of the load current. However, the operating pressure trends were almost stable for the entire period, except for the moments of temporary vacuum that were executed just for the BPR testing and not for simulating the actual flight condition.

4.2. Demonstration flight

A large balloon, B50-50, equipped with the fuel cell system was launched from SBC on August 30th, 2007 at 6:02. The fuel cell system performance data obtained during the demonstration flight is shown in Fig. 9.

After the fuel cell stack was purged with nitrogen for approximately 5 min, the reactants were introduced at 5:03. When the reactants were supplied, the open-circuit voltage increased to 14.9 V. At 5:07, the fuel cell stack started generating a load current of 2 A after attaining a stable voltage. At 5:12, the flow rates of the reactants were increased, and the load current was increased to 4 A at 5:17. After the startup of the fuel cell stack, all the instruments were begun to be powered by the fuel cell by switching power relays. The fuel cell power generation was approximately 50 W. Variations in the flow rates and load current before the launch were caused by the command tests. The external power supply and non-flight gas cylinders were separated at 5:24 and 5:25, respectively, and the fuel cell system shifted to a self-operating mode that was supplied with power and gas from its own system. The B50-50 balloon was launched at 6:02 after a 30 min helium filling operation. Flow rates of reactants and load current were increased at 8:00 and 8:03, respectively, by sending commands. The fuel cell power generation was approximately 80 W. Residual gases in the cylinders were released by sending commands at 8:55 so as to end the demonstration flight.

The individual cell voltages are shown at the top of Fig. 9. As the operating pressure decreased with the balloon ascent, stack and cell voltages decreased slightly. Voltage of Cell 16, which had always shown the worst trend prior to the flight, was significantly low compared with the voltage of other cells when the load current flowed. Although there were some deviations, there was probably no severe flooding, because cell voltages were almost stable during the flight.

The operating pressure of the fuel cell stack was approximately 200 kPa on the ground. It gradually decreased with the altitude

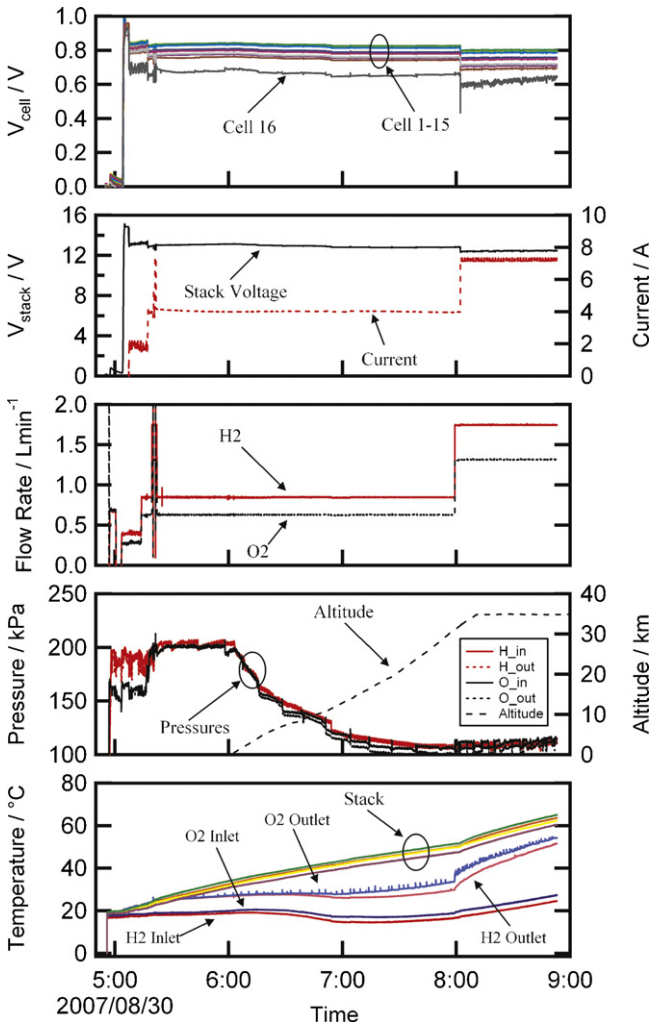

Fig. 9. Performance of the fuel cell system during the demonstration flight. From the top to the bottom, cell voltage, stack voltage or load current, flow rate, pressure or altitude, and temperature are plotted.

and hovered at around 100 kPa after the balloon reached the target altitude of 35 km, as shown in the second figure from the bottom in Fig. 9. This indicated that there was no blockage of the flow passages by frozen product water which could be detected by unexpected increases in the operating pressure. When the balloon was rising, the inlet and outlet pressures of oxygen showed steep periodic decreases, whereas the anode pressures, i.e., the inlet and outlet pressures of hydrogen decreased relatively smoothly. This phenomenon was not observed in the ground test, because a slow decrease in the ambient pressure simulating the balloon ascent was not performed. The periodic steep decreases in oxygen pressures could be attributed to an intermittent plugging of oxygen flow passages with product water after the outlet of the fuel cell stack, because both the inlet and outlet pressures of oxygen varied simultaneously. Water is produced at the cathode, and it is mainly exhausted from the cathode side. BPRs had an orifice to control operating pressure, and were placed after the outlets of the fuel cell stack. The scenario of the periodic steep decreases in the cathode pressure can be explained as follows. First, product water was mainly exhausted from the cathode and was accumulated in the BPR in the form of water droplets that hindered the BPR operation. Second, the differential pressure between the inlet and outlet of the BPR increased with altitude, because the water droplets prevented the BPR from tracking decreases in ambient pressure. Third, an increased differential pressure of the BPR blew off the water droplets, and the BPR immediately caught up with the decrease in ambient pressure. This immediate catching up is presumably the cause of the steep decrease in cathode pressure.

Fluctuations in pressures after 8:00 were probably due to an increase in the production rate of water with an increase in the load current; but, this kind of pressure variation was not observed in the ground test, even though the load current was identical, as shown in Fig. 8. It is assumed that the oxygen outlet temperature had a significant effect on the pressure variations. The oxygen outlet temperature for the ground test was in the range 40–60 °C and 60–67 °C for load currents of 4 and 8 A. On the other hand, during the flight, that temperature was in the ranges 20–30 °C and 30–55 °C before and after increasing the load current, respectively. In general, low temperatures help the membrane in maintaining its hydration level high enough, because the saturated vapor pressure is low at low temperature. This indicates that lower the temperature, greater is the condensation of the product water. The low-temperature condition in the flight was prone to produce more condensed product water than in the ground test. The condensed product water could form water droplets affecting the operating pressures by an alternate plugging up and blowing off in the flow passages after the fuel cell stack. Since the piping and manual valves have wide flow passages, the check valve and BPR are the presumable places where the water droplets caused these problems. In particular, the BPR, having an orifice to control its back pressure, was the most likely candidate.

The exhaust gas passing through the check valve and the BPR possibly included not only water droplets but also iced particles if there were local cold spots due to incomplete thermal insulation for exhaust piping. Liquid water droplets have surface tension, so that they can easily block the flow passages. And the blockage can be also removed easily by the reactant flow. On the other hand, small iced particles are deduced to block only when they accumulate and grow into larger particles than the flow passages. A blockage with large iced particles is speculated to be detected as an abnormal continuous pressure rise because they can be removed only by thawing. There was no way to detect existence of small iced particles, but it is conjectured that they immediately thawed at resulted temperature of the outlet gas (25–30 °C) or passed through the passages without affecting unless they accumulated and grew. Therefore, the combination of water droplets and the BPR or check valve could be considered as possible causes for the oxygen pressure variations.

The periodic steep decreases and variations in oxygen pressures did not seem to affect the overall performance of the fuel cell system. However, the cell voltages showed slight variations in synchronizing with the oxygen pressures, as shown in Fig. 10, which illustrates the cell voltages, pressures, and temperatures. Slight variations in voltage that were induced by oxygen pressure spikes would be a non-negligible noise source in particular scientific applications that use noise-sensitive instruments. This suggests that the mechanism of generating pressure spikes should be understood for a better design that improves the fuel cell stability. The phenomenon of pressure spike generation will be discussed in detail in the following section.

Temperatures of the fuel cell stack and outlet gases were gradually increased by the generated heat, especially after increasing the load current at 8:00, as shown at the bottom of Fig. 9. The temperatures of the outlet gases, which had been warmed while traveling through the fuel cell stack, were higher than those of the inlet gases. Slight variations in the oxygen outlet temperature were frequently observed, especially after increasing the load current. These frequent variations were probably due to an intermittent exhaustion of water droplets coming out from the fuel cell stack, because some of these temperature variations synchronized with the variations in the oxygen pressure as shown in Fig. 10. This suggests

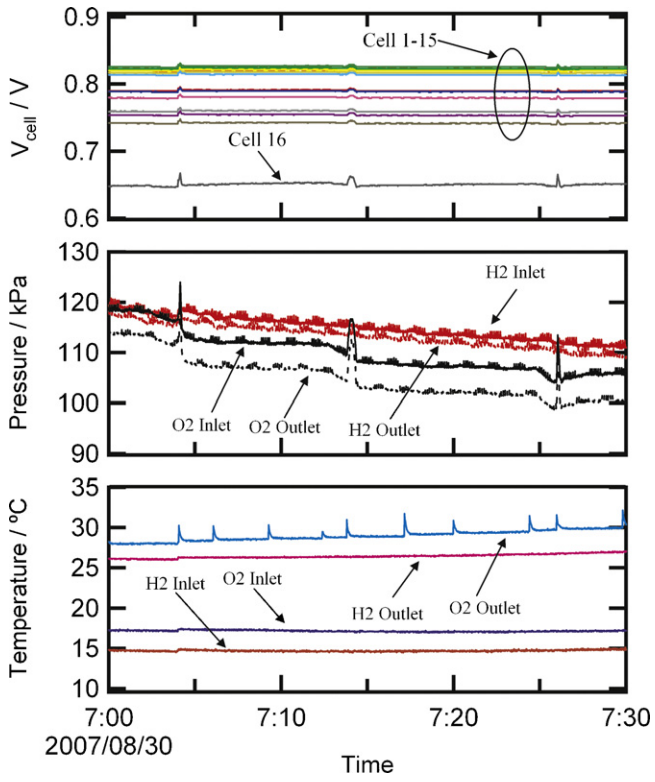

Fig. 10. Magnifications of cell voltage, pressure, and temperature of the fuel cell system during the demonstration flight.

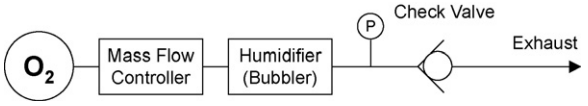

Fig. 11. Experimental setup for the check valve characteristic test.

that some of the water droplets expelled from the fuel cell stack could directly act as triggers causing plugging. The synchronized temperature variations support the pressure variation mechanism caused by the combination of water droplets and the BPR or check valve.

4.3. Characteristics of check valve and back pressure regulator containing water droplets

The most probable cause of oxygen pressure variation, which was often observed in the flight, is a combination of water droplets and the check valve or BPR, as mentioned in the previous section. Post-flight experiments, using the setups shown in Figs. 11 and 12, were performed to identify the characteristics of check valves and BPR containing water droplets. The check valve (Swagelok SS-CHS4-1, 1 psig) and the BPR (TESCOM, 44-47, 50 psig) were same as those used in the flight. Oxygen with a flow rate of 890 ml min^{-1}, which was same as the increased outlet flow rate in the flight, was supplied to the check valve or BPR through a bubbler humidifier. The humidification temperature was 80 °C that was high enough to produce an adequate amount of water droplets. The secondary side of the BPR

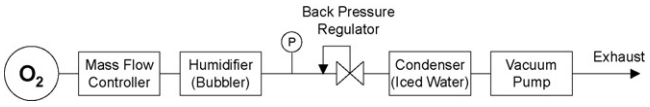

Fig. 12. Experimental setup for the back pressure regulator characteristic test.

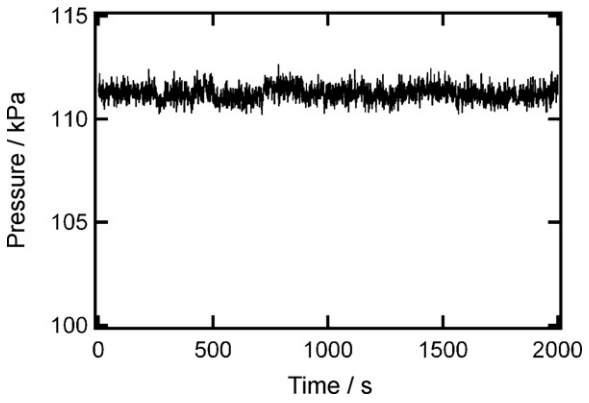

Fig. 13. Characteristic of the check valve containing water droplets.

was evacuated by the vacuum pump via an iced water condenser whose function was to remove water droplets and protect the vacuum pump. The primary pressure was set at about 105 kPa by the BPR. The vacuum pump was disabled, and the BPR was fully opened to differentiate its characteristics with and without regulation.

The check valve showed very stable characteristics, as shown in Fig. 13, proving that the check valve was not the cause of pressure variations. On the other hand, BPR showed periodic large pressure spikes, as shown in Fig. 14(a), when it was regulating and the secondary side was evacuated. As shown in Fig. 14(b), when the BPR was fully opened and the vacuum pump disabled, there were spikes, but they were quite smaller. In general, a BPR controls its primary pressure by throttling its orifice where the water droplets are prone to plug the flow passage. The flow passage narrows to a greater extent when the BPR is regulating compared with when it is fully opened. The narrowed flow path for controlling the primary pres-

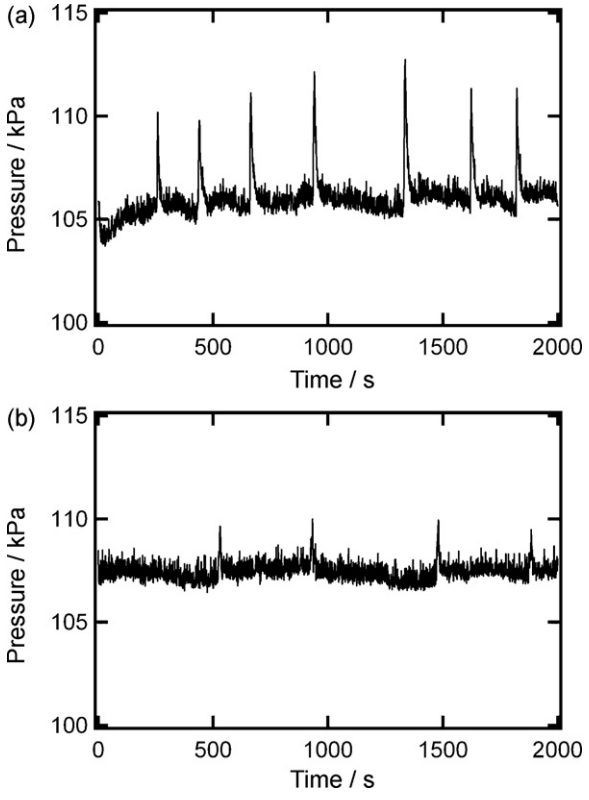

Fig. 14. Characteristics of the back pressure regulator containing water droplets. (a) The BPR regulating and (b) the BPR fully opened.

sure was assumed to be more prone to accumulating water droplets that caused the periodic large pressure spikes.

These results indicated that the fuel cell system works better when the exhausting product water is in vapor form rather than in the liquid form, because this avoids a periodic plugging of the flow passage of the BPR. Decreasing relative humidity of the exhaust gas is a key of vapor form exhaustion, and this can be achieved by increasing temperature and/or reactant flow rate at a given pressure. Increasing temperature of the exhaust gas by heating the piping is preferable to increasing flow rate resulting in poor reactant utilization. Besides, it is better if the BPRs are installed considering the gravity that would capture the water in the piping and the BPR so that the amount of water is as less as possible to realize a stable performance.

5. Conclusions

Non-external humidified fuel cell system was developed for high-altitude balloons. The ground performance test, simulating high-altitude vacuum conditions, was performed before the flight. A demonstration flight of the fuel cell system was launched using a large balloon to verify its performance under actual high-altitude conditions. The fuel cell system showed an almost stable performance during the demonstration flight. However, slight variations in the oxygen pressure affecting the cell voltages were observed. Post-flight experiments identifying characteristics of the check valve and BPR confirmed that the pressure variations were probably caused by an intermittent water plugging of the flow passages in the BPR. The results of the demonstration flight indicated that the operating conditions in which the fuel cell stack exhausts product water in the form of vapor and not in the liquid form, were preferable to realize a more stable performance. Vapor form exhaustion can be achieved by decreasing relative humidity of the exhaust gas with increasing temperature and/or flow rate. Installation of BPRs is better to be considered to prevent an accumulation of water droplets in the system.

Acknowledgments

The authors would like to thank Japan Society for the Promotion of Science, and the New Energy and Industrial Technology Development Organization of Japan for financial support of this work.

References

[1] L.N. Rey, J. Mosquera, E. Bataller, F. Orti, C. Dudfield, A. Orsillo, J. Power Sources 181 (2008) 353–362.
[2] V. Chang, J. Gallman, SAE Trans. 113 (1) (2004) 1943–1957.
[3] F. Barbir, T. Molter, L. Dalton, J. Hydrogen Energy 30 (2005) 351–357.
[4] H. Oman, IEEE AESS Systems Magazine (2002) 35–41.
[5] J. Larminie, A. Dicks, Fuel Cell Systems Explained, second ed., Wiley, Chichester, England, 2003, pp. 80–82.
[6] Y. Sone, Y. Ariyama, M. Uno, H. Naito, H. Ino, Electrochemistry 75 (2) (2007) 197–200.
[7] K.M. Williams, R.H. Kunz, M.J. Fenton, J. Power Sources 135 (2004) 122–134.
[8] Y. Sone, M. Ueno, S. Kuwajima, J. Power Sources 137 (2004) 269–276.
[9] Z. Qi, A. Kaufman, J. Power Sources 109 (2002) 469–476.
[10] J.R. Spiegel, T. Gilchrist, E.D. House, Proc. Inst. Mech. Eng. Part A: J. Power Energy 213 (1) (2004) 57–68.
[11] W.J. Pratt, J. Brouwer, S.G. Samuelsen, J. Propul. Power 23 (2) (2007) 437–444.
[12] Y. Sone, M. Ueno, H. Naito, S. Kuwajima, J. Power Sources 157 (2006) 886–892.
[13] F. Barbir, H. Gorgun, J. Appl. Electrochem. 37 (2007) 359–365.
[14] M. Kim, J.Y. Sohn, W.C.Y.W. Lee, S.C. Kim, J. Power Sources 176 (2008) 529–533.
[15] I. Johnston, Pressure Regulators Explained, TESCOM Technical Training, http://www.tescom-europe.co.uk/fileadmin/user_upload/Tescom_UK/.